Journal of Applied Ichthyology

J. Appl. Ichthyol. 31 (Suppl. 4) (2015), 88–97

ISSN 0175–8659

Received: June 22, 2015
Accepted: October 14, 2015
doi: 10.1111/jai.12983

Description of the skeletal anatomy of reared juveniles of *Pseudoplatystoma punctifer* (Castelnau, 1855) with notes on skeletal anomalies

By G. Estivals[1], C. García-Dávila[2] and M. J. Darias[1]

[1]*Institut de Recherche pour le Développement, Unité Mixte de Recherche Biologie des Organismes et Ecosystèmes Aquatiques (UMR BOREA - MNHN, CNRS-7208, UPMC, UCBN, IRD-207), Montpellier, France;* [2]*Instituto de Investigaciones de la Amazonía Peruana, Programa de Investigación para el Uso y Conservación del Agua y sus Recursos, Iquitos, Peru*

Summary

This study aimed at describing the normal bony skeleton of *Pseudoplatystoma punctifer* juveniles to use as a reference when assessing the adequacy of nutritional and environmental conditions in experimental rearing during the early developmental stages and to provide a baseline for characterizing skeletal anomalies that might appear in rearing trials with this species. Fertilized eggs and newly hatched *P. punctifer* larvae were incubated at 27.8 ± 0.4°C in two 60-L tanks (50-L water volume) connected to a clear water recirculating system. At 3 days post fertilization – dpf (2 days post hatching – dph) larvae were reared in three 40-L tanks (30-L water volume; initial n = 2700 larvae per tank; 28.3 ± 0.4°C, pH 6.9 ± 0.2, dissolved oxygen 8.2 ± 0.5 mg L^{-1}, $N–NO_2$ 0.04 ± 0.02 mg L^{-1}, $N–NH_4$ 0.14 ± 0.05 mg L^{-1}; 0L:24D photoperiod) and fed as follows: non-enriched *Artemia* spp. nauplii from 4 to 21 dpf (3–20 dph) and a commercial compound diet from 18 dpf onwards. *Pseudoplatystoma punctifer* juveniles (23.2 ± 5.5 mm standard length, SL, n = 58) were stained with alizarin red and their skeletal structures analysed and identified under stereoscope. *Pseudoplatystoma punctifer* presents an osseous skeleton typical of catfishes, consisting of a broad and depressed skull containing small eyes, 43–44 vertebrae (44 being the most frequent), a caudal fin complex composed of one epural, five hypurals, one parhypural and two hypurapophyses, dorsal and pectoral fins with spines and anal and adipose fins. The observed occurrence of several skeletal anomalies indicates that the rearing conditions might have been suboptimal.

Introduction

The skeletal system of fish responds very sensitively to changes in environmental and nutritional conditions, in particular during early developmental stages. So far, little is known about the incidence of skeletal anomalies in farmed Amazonian fish species (Fujimoto and Carneiro, 2008; Fujimoto et al., 2013; Lopes et al., 2014). However, skeletal anomalies are a major problem in cultured teleost fishes and cause economic, biological and ethical issues. For instance, losses in the European aquaculture industry due to deformed fish are estimated to be in excess of 50,000,000 € per year, thus a reduction in skeletal abnormalities would greatly improve production (Boglione et al., 2013a). Abnormalities mostly appear during larval development and early juvenile stages, when various differentiation patterns evolve in the process of morphogenesis (Divanach et al., 1996; Boglione et al., 2013a,b) and molecular pathways involved in skeletal ontogenesis could be altered (Darias et al., 2011a). Many factors such as physiological, environmental, genetic, xenobiotic and nutritional can affect this process (Cahu et al., 2003; Lall and Lewis-McCrea, 2007; Darias et al., 2011a; Boglino et al., 2013; Boglione et al., 2013a,b). Therefore, analysis of the skeletal system at early stages of fish development is a useful marker when assessing the rearing conditions (i.e. environmental and nutritional) of individuals.

Pseudoplatystoma punctifer is a commercially important catfish species for human consumption in Amazonia and presents a high potential for aquaculture (Kossowski, 1996). Belonging to the family Pimelodidae and the order Siluriformes, the genus *Pseudoplatystoma*, whose known distribution includes the major river basins of South America, was initially composed of three species; the latest systematic revision recognizes eight species, based on body shape, colour pattern, skeletal anatomy, and vertebral numbers (Buitrago-Suárez and Burr, 2007). In terms of skeletal characteristics, for example, *P. punctifer* differs from *Pseudoplatystoma fasciatum* in the vertebra number where the first spinelet of the anal fin contacts the haemal arch and in the number of vertebrae (Buitrago-Suárez and Burr, 2007). Several anatomical skeletal elements have been described for the species of the genus *Pseudoplatystoma* (see Buitrago-Suárez and Burr, 2007) but to our knowledge no detailed description of the skeletal anatomy of *P. punctifer* is available in the literature.

Pseudoplatystoma punctifer has a short larval development of around 2 weeks from fertilization (Gisbert et al., 2014) and a promising potential for growth (Darias et al., 2015). However, knowledge on the most suitable rearing conditions, especially the nutritional requirements, during the early stages of development is limited (Darias et al., 2015). Several skeletal anomalies have been observed in adults as well as in early life stages of this species, suggesting that rearing protocols need to be improved to reduce these inci-

dences (Estivals et al., 2015). Therefore, the aim of the present study was to describe the normal anatomical features of the bony skeleton of *P. punctifer* in order to use it as reference when assessing the adequacy of nutritional and environmental conditions in experimental rearing during the early stages of development and to provide a baseline for characterizing skeletal anomalies that might appear in rearing trials with this species.

Fig. 1. Juveniles of *Pseudoplatystoma punctifer*, lateral view. (a) Fixed in 4% neutral buffered formalin, 22 mm SL. (b) Coloured with alizarin-red, 18 mm SL. Both reared at 28.3 ± 0.4°C

Materials and methods

Newly hatched *P. punctifer* larvae were obtained by hormonal induction as described in Gisbert et al. (2014), of a sexually mature pair of *P. punctifer* (♀: 4.73 kg; ♂: 1.15 kg) from a broodstock maintained in captivity at the Instituto de Investigaciones de la Amazonía Peruana (IIAP, Iquitos, Peru). Stripping of the female, sperm collection and fertilization procedure was performed following the protocol described by Nuñez et al. (2008). Spawned eggs (fertilization rate = 90%; hatching rate = 84%, 18 ± 2 h after fertilization) were incubated at 27.8 ± 0.4°C in two cylindroconical 60-L tanks (50-L water volume) connected to a clear water

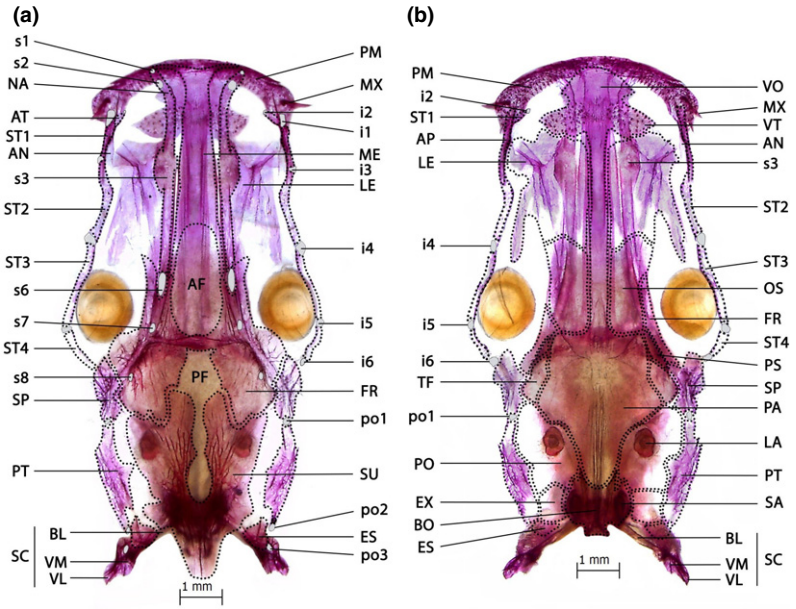

Fig. 2. Cranium of *Pseudoplatystoma punctifer*, 28 mm SL (reared at 28.3 ± 0.4°C). (a) Dorsal view. (b) Ventral view. FR, SU, PT and SP joined to each other by several sutures. The cranial fontanels completely opened and separated by a conspicuous epiphyseal bar; AF oval-shaped and shorter and wider than PF (more irregular shaped). Antero- and posterolateral *cornua* of ME narrow-shaped. Border shape of ME roughly straight and regular. LE (accommodates the olfactory organ) wide and weakly ossified. Posterior portion of LE sheet-shaped and more developed than the anterior one. Posterolateral corner of the LE elongated and reaches the eyes. Joint between LE and OS inconspicuous. Lateral margin of FR slightly concave. SP weakly ossified and two times smaller than PT. NA long, thin, spongy and straight from the s2 to s6 and wider at s3 region. AN rod-like and with dorsomedial lamina weakly ossified. i bone series parallel to the s ones with a concavity at ST2 level and a convexity at the eyes region. AT transversally attached to the dorsal surface of the anteromedial portion of the AN. ST1 obliquely attached to the dorsal surface of the anterolateral portion of the antorbital bone. Posterior end of ST4 joined to the SP. ES triangular, transversally oriented and attached to posterolateral region of the cranium. SU process large and long, without crest and covers the EX and BO. Anterior part of SU divided into two branches, both also divided into another two ramifications. EX only visible transversally. VO elongated and expanded anteriorly. Two VT (30–40 teeth each) fused to the VO posteriorly and to the PA ventrolaterally. TF large, anteroposteriorly elongated and bordered by the PS anteriorly and anterodorsally, by SP laterodorsally, PA lateroventrally and PO posteroventrally. AP thin and elongated and superposed to the ST1 and the anterior part of the ST2. Paired PM triangular, short and narrow (100–110 teeth each). Paired MX small and triangular. Proximal extremity of BL completely ossified except for the portion attached to the BO and EO. BL roughly straight and co-ossified with the SC. Dorsolateral limb SC slightly concave ventrally and attached dorsolaterally to ES. VL and VM distally unconnected. AF, anterior fontanel; AN, antorbital; AP, autopalatine; AT, antorbital tubule; BL, Baudelot's ligament; BO, basioccipital; ES, extrascapula; EX, exoccipital; FR, frontal; i1-6, infraorbital sensory branches 1–6; LA, lapillus; LE, lateral ethmoid; ME, mesethmoid; MX, maxilla; NA, nasal; OS, orbitosphenoid; PA, parasphenoid; PF, posterior fontanel; PM, premaxilla; PO, prootic; po1-3, postotic sensory branches 1–3; PT, pterotic; PS, pterosphenoid; SA, sagittae; SC, supracleithrum; SP, sphenotic; ST1-4, suborbital tubules 1–4; SU, supraoccipital; s1-3, supraorbital sensory branches 1–3; s6, supraorbital sensory branch 6 (epiphyseal branch); s7, supraorbital sensory branch 7 (postorbital branch); s8, supraorbital sensory branch 8 (parietal branch); TF, trigeminofacial foramen; VL, ventrolateral limb of supracleithrum; VM, ventromedial limb of supracleithrum; VO, vomer; VT, vomeral teeth plate. Dotted lines delimit structures

recirculating system. Larvae were transferred at 3 dpf (2 dph, 5.6 mm total length, TL) into three 40-L tanks (30-L water volume, initial n = 2700 larvae per tank) and reared at 28.3 ± 0.4°C and total darkness (water conditions: pH 6.9 ± 0.2, dissolved oxygen 8.2 ± 0.5 mg L^{-1}, $N–NO_2$ 0.04 ± 0.02 mg L^{-1}, $N–NH_4$ 0.14 ± 0.05 mg L^{-1}). Water temperature, pH and dissolved oxygen were measured daily and $N–NO_2$ and $N–NH_4$ weekly at 07.00 h in the three tanks. Water supply was adjusted in each tank to assure a water flow rate of 0.2 L min^{-1}. Larvae were fed six times a day from 4 to 21 dpf with non-enriched *Artemia* spp. nauplii in slight excess (0.4–17 nauplii ml^{-1}) considering the larval density, the weight increase of the larvae and the daily food ration (Baras et al., 2011) as well as with a commercial diet (BioMar®, Nersac, France; proximate composition: 58% proteins, 15% lipids, 11% ash; particle size: 0.5 mm) from 18 to 32 dpf. Once weaned (22 dpf), larvae were fed five times a day at 5% of the larval wet weight. Fifty-eight juveniles of 23.2 ± 5.5 mm standard length (SL) were sampled, anaesthetized using Eugenol (0.05 μl ml^{-1}; Moyco®, Lima, Peru), fixed in 4% neutral buffered formalin and stored at 4°C.

In order to describe the bony elements of the skeleton, fish were stained with alizarin red according to Darias et al. (2010a). Briefly, individuals were washed in distilled water and subsequently treated in a bleaching solution containing H_2O_2 for 1 h. A clearing step was not necessary. Specimens were then transferred to a bone staining solution containing alizarin red (SIGMA T4799) and incubated for 20 h. Individuals were washed thereafter and dehydrated with increasing series of glycerol. Skeletal structures were analysed under stereoscope and identified and named according to Bockmann and Castro (2010) and Faustino and Power (2001). Photos were taken with a Leica camera (EC3, firmware:

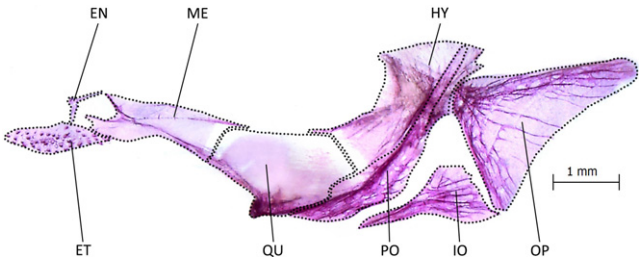

Fig. 3. Left suspensorium and opercular series of *Pseudoplatystoma punctifer,* 28 mm SL (reared at 28.3 ± 0.4°C), lateral view. EN bracket-shaped and attached by ligaments posteriorly to the anterior edge of MT, anteriorly to LE (not shown in figure) and reaches ventrally the ET approximately posteromedially. ET (30–40 teeth) fused posteroventrally with ME. ME joined to QU synchondrally medioposteriorly and interdigitally ventrally. ME fused synchondrally to QU posteriorly forming a convex structure. Dorsal part of ME joins QU anterolaterodorsally. QU joined posteriorly to HY synchondrally and attached posteroventrally to PO. Anterodorsal part of HY joins QU posterodorsolaterally. ME and HY separated by cartilage at dorsal part of QU level. Anterodorsal margin of HY with bony outgrowths. HY attached lateroventrally to PO. Subpreopercle and suprapreopercle ossicles absent. OP large, triangular, with shelf-like projections mostly present laterodorsally and lateroventrally while lateral surface mostly smooth. IO triangular, narrow and elongated from the middle to the anterior part (with shelf-like projections). PO, concave mediolaterally, articulates with the ventral margin of the QU anterodorsally and posterodorsally and with the anteroventral border of the HY. EN, entopterygoid; ET, ethmoid teeth plate; HY, hyomandibula; IO, interopercle; LE, lateral ethmoid; ME, mesethmoid; MT, metapterygoid; OP, opercle; PO, preopercle; QU, quadrate. Dotted lines delimit structures

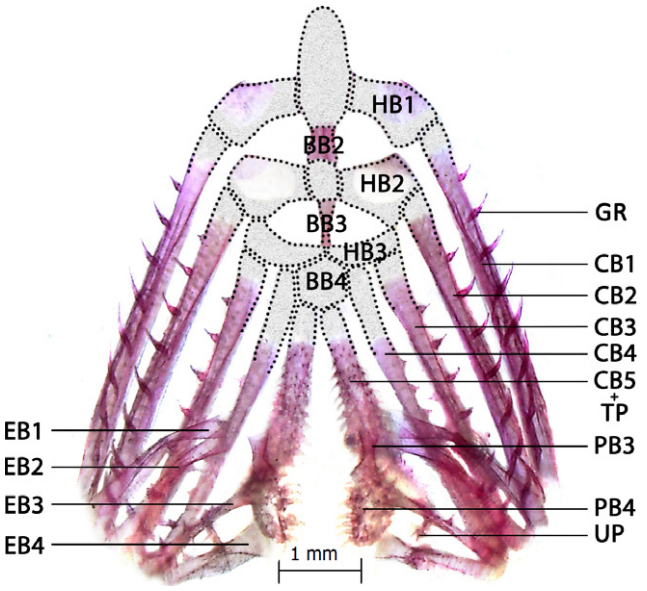

Fig. 4. Branchial arches of *Pseudoplatystoma punctifer*, 28 mm SL (reared at 28.3 ± 0.4°C), dorsal view. CB and EB support a series of GR. BB1 absent or not calcified yet for the studied size classes of fish (23.2 ± 5.5 mm SL). BB2 ossified, BB3 weakly ossified and BB4 is a non-ossified (cartilaginous) hexagonal plate dorsally that turns oval ventrally. Paired HB1 fused laterally to the cartilaginous part of BB2. Paired HB2 fused laterally to the cartilaginous part of BB3. Paired HB3 fused together and HB3 junction fused dorsally to the posterior part of BB3. HB1 and HB2 weakly ossified, paired HB3 not ossified and HB4 absent. CB1 joins the posterodistal cartilage region of HB1 at its posteromiddle outer margin. Anterodistal margins of paired HB1 with discrete osseous prominences (uncinate process absent). HB2 slightly wider than HB1 and weakly ossified and cartilaginous posteriorly and at extremities. CB2 joins the posterodistal cartilage region of HB2 at its posteromiddle outer margin. Anterodistal region of HB2 has a slightly oriented process. CB largely ossified except at extremities. CB and EB with a series of long, spaced and curved GR that progressively become short and regular from CB1-EB1 to CB4-EP4. CB1 the longest and CB2 and CB3 similar in length and width. CB1 to CB4 slightly curved mediodorsally (more pronounced in CB4). This region seems to be strangled and fused with shelf projections oriented to the extremities. Proximate cartilaginous head of CB4 long and laterally straight. TP posteromedially expanded, covers the dorsal and inner lateral part of CB5 and presents long 100–110 conical teeth posteriorly oriented. Longer GR in the external part of CB3, very small GR in the inner part of CB4. EB1 to EB4 rod-like and largely ossified except at extremities. Medial border of EB3 with an UP reaching EB4. EB4 posteromedially strangled from where broad crests are developed. EB5 very thin, when present, the posterior part being cartilaginous, and positioned ventrolaterally to EB4 and fused anteriorly to EB4 medioventrolaterally (not shown in figure). PB1 and 2 absent. PB3 rod-like, widely ossified (except at extremities) and with shallow crests and expanded extremities, especially the posterior one. PB4 mostly oblong, compressed laterally and slightly ossified. Accessory cartilaginous nodule between the inner tips of EB1 and EB2 and the anterior extremity of PB3. The upper pharyngeal TP oval, disposed lateroventrally to PB and composed of large and conical teeth. BB2-4, basibranchials 2–4; CB1-5, ceratobranchials 1–5; EB1-5, epibranchials 1–5; GR, gill raker; HB1-3, hypobranchials 1–3; PB3-4, pharyngobranchials 3 and 4; TP, tooth plate; UP, uncinate process. Dotted lines delimit structures. Greyish areas represent cartilage

1.9.44) connected to a Leica stereoscope (M125) and processed using Leica LAS EZ 3.0.0 (Leica Microsystems, Wetzlar, Germany), IMAGEJ (Rasband, 1997–2012, v1.49) and PHOTOSHOP CC (Adobe Systems, Inc., San Jose, CA) software.

Results

Head skeleton

Cranium, suspensorium and opercular series. The cranium of *P. punctifer* juveniles is dorsoventrally flattened and elongated anteriorly (Fig. 1). Cranial roof bones are smooth and without any ornamentation (Fig. 2). The bony interorbital width is broad and the orbital region is visible from a dorsal view, the posterior inner part of the eyes being covered by the outer border of the frontal. The infraorbital laterosensory canal is composed of five paired tubular ossifications: one antorbital and four suborbitals tubules. The post-temporal is very prominent and plated on the exoccipital, reaching to the posterolateral part of the supraoccipital and fused with the scapula. The extrascapula is juxtaposed to the post-temporal and superposed to the epioccipital. The optic nerve foramen is large and circular and delimited by the orbitosphenoid anteriorly, the parasphenoid ventroposteriorly and the pterosphenoid dorsolaterally. The paired dentary are spongy, smooth and attached to each other by a ligament. The dentary (85–95 teeth each) are fused posteriorly to the anguloarticular by interdigitations and posterodorsally to the ventral margin of the anguloarticular and the retroarticular. The dentary exceed posteriorly the articular and is condyle-like shaped. The anguloarticular is wide, triangular and presents shelf-like projections. The coronomeckelian cartilage is triangular and fused with the inner part of the dentary-anguloarticular suture. The coronomeckelian bone is discoid and fused with the coronomeckelian cartilage at its inner lateral part and is located at the medial part of the dentary-anguloarticular suture. The suspensorium, described in Fig. 3, includes the endopterygoid, metapterygoid, hyomandibular and quadrate.

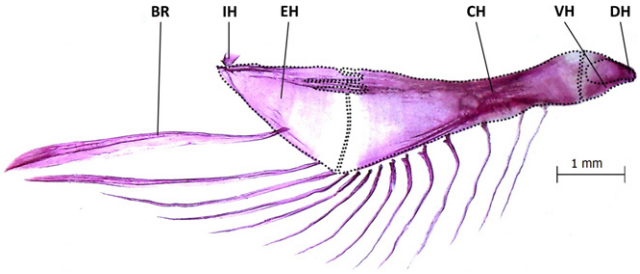

Fig. 5. Right hyoid arch of *Pseudoplatystoma punctifer*, 28 mm SL (reared at 28.3 ± 0.4°C), medial view. Lateral surface of hyoid arch convex with conspicuous shelves from anterior to midlength portion of CH. Posterior portion of H and anterior portion of CH expanded. DH weakly ossified and fused through shelf projections to anterior part of VH. CH anteriorly joined synchondrally to H and posteriorly to EH (joint synchondrally medioventrally and interdigitally dorsoposteriorly). Hyoid arch with 13–15 BR (14 most frequent, Table 1): 10 placed on ventral border of CH, 2 on inter-EH-CH cartilaginous joint, and 2 ventral border of EH. Urohyal (not shown in figure) triangular and with dorsal keel reaching approximately to posterior part of CH. The IH attached dorsally to ventromedial part of hyomandibular by a ligament (not shown in figure). BR, branchiostegal ray; CH, ceratohyal; DH, dorsal hypohyal; EH, epihyal; H, hypohyal; IH, interhyal; VH, ventral. Dotted lines delimit structures

Branchial arches and hyoid arch. The complex of branchial arches is formed by the lower (basibranchials, cerato-

Table 1
Descriptive meristic, location and frequency of items of the normal skeleton of reared *Pseudoplatystoma punctifer* juveniles (23.2 ± 5.5 mm SL; rearing temperature 28.3 ± 0.4°C, n = 10)

	Number	Frequency (%)
Hyoid arch		
Branchiostegal rays	13	10
	14	80
	15	10
Axial skeleton		
Vertebrae	44	70
	43	30
Parapophyses	11	90
	12	10
First complete haemal spine on vertebra	16	90
	17	10
Appendicular skeleton		
Pectoral fins		
Fin rays	8	80
	9	20
Dorsal fin		
Pterygiophores	7	90
	8	10
Fin rays	6	90
	7	10
Location of the proximal tip of the last pterygiophore		
Between the pseudoneural spines of v9 and 10		50
At the level of the pseudoneural spine of v9		40
At the level of the pseudoneural spine of v10		10
Anal fin		
Location of the proximal part of the first pterygiophore		
Between haemal spines of v23 and 24		20
Between haemal spines of v24 and 25		50
Between haemal spines of v25 and 26		10
Reaching haemal spine of v24		10
Reaching haemal spine of v25		10
Location of the proximal part of the last pterygiophore		
Between haemal spines of v33 and 34		20
Between haemal spines of v34 and 35		20
Reaching haemal spine of v34		60
Adipose fin		
Location of the anterior part		
Above v24		30
Above v25		10
Above v26		20
Above v27		20
Above v28		20
Location of the posterior part		
Above v34		60
Above v35		10
Between v34 and 35		30

v, vertebra.

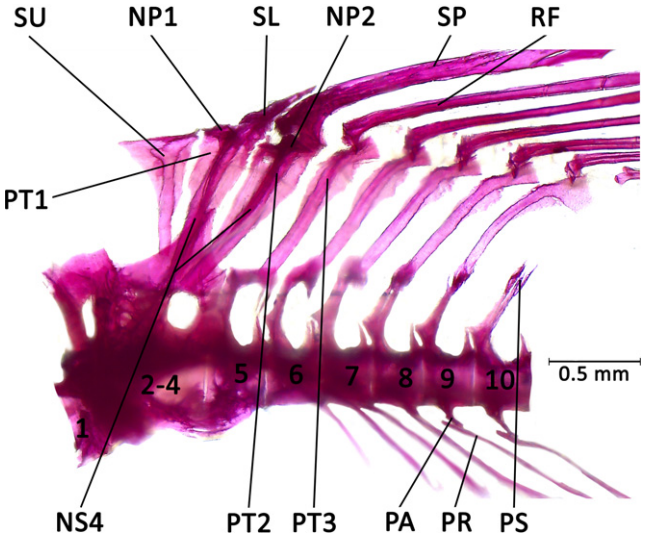

Fig. 6. Weberian apparatus and dorsal fin of *Pseudoplatystoma punctifer*, 28 mm SL (reared at 28.3 ± 0.4°C), lateral view. SU triangular shaped and connected ventroposteriorly to NP of vertebra 3. PT1 and 2 adjacent and distally sutured. Distal extremity of PT1 expanded to form NP1. NP1 posterodorsally articulated with the SL and ventroposteriorly connected to the bifid NS4. Distal extremity of PT2 expanded anterolaterally to form NP2. NP2 posterodorsally articulated with the rigid SP and ventroposteriorly connected to the bifid NS4. NP1-2, nuchal plates 1 and 2; NS4, neural spine 4; PA, parapophysis; PR, pleural ribs; PS, pseudoneural spine; PT1-3, pterygoiphores 1–3; RF, ray fin; SL, spinelet; SP, pectoral spine; SU, supraneural

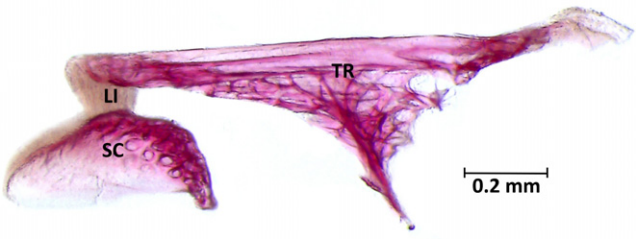

Fig. 7. Weberian apparatus of *Pseudoplatystoma punctifer*, 28 mm SL (reared at 28.3 ± 0.4°C), ventral view. SC wide patelliform shaped and attached mediolaterally to TR by a ligament. Intercalarium absent. TR triangular and laterally attached with a spatula to the complex vertebra and posteriorly to the swim bladder (large, transversely bilobed, giving dorsally a heart-shape aspect, foreshortened to the anterior body cavity and extended posteriorly until the vertebra 9). LI, ligament; SC, scaphium; TR, tripus

branchials and hypobranchials) and upper (epibranchials and pharyngobranchials) branchial arches. The hyoid arch is composed of ceratohyal, epihyal, hypohyal and interhyal, and branchiostegal rays. Branchial arches and hyoid arch are described in Figs 4 and 5, respectively. The number of branchiostegal rays is indicated in Table 1.

Axial skeleton

Weberian apparatus. The anterior vertebrae are shown in Fig. 6. The *centrum* 1 is autogenous, disc-like and firmly attached to the basioccipital and the complex vertebra (vertebrae 2–4). The joint between the complex vertebra and the vertebra 5 is interdigitated; the joint between the remaining vertebrae is symphyseal. The dorsal margin of the vertical lamina of the complex vertebra is weakly developed. The neural spine of the vertebra 4 forms an angle of approximately 135° (134.9 ± 4.1°, n = 10) with the axe of the column; from the medial to the distal part the angle is inclined to approx. 126° (126.2 ± 2.7°, n = 10) reaching the anterior portion of the neural spine of the vertebra 5 (Fig. 6). The transverse process of the vertebra 4 is clearly divided into anterior and posterior branches on some specimens. In others, the anterior branches seem to be absent or weakly developed, or the anterior and posterior branches are weakly divided, or without the left anterior branch. When present, the anterior branches of the transverse process of the vertebra 4 are wide and ventrolaterally oriented. The distal portion of the posterior branches of the transverse process of the vertebra 4 is laminar, wider than the anterior branches and lateroposteriorally expanded. The anterior portion of the posterior branches of the transverse process of the vertebra 4 presents a spatula form in its distal part. The posterior portion of the posterior branches of the transverse process of the vertebra 4 is triangular. The posterior border of the anterior branches and the anterior margin of the arborescent portion of the posterior branches of the transverse process of the vertebra 4 are joined via a bony bridge-like element. The transverse process of the vertebra 5 presents pleural ribs.

Other elements of the Weberian apparatus are described in Fig. 7.

Vertebral column and caudal fin complex. The vertebral column is composed of a variable number of vertebrae, 44 being the most frequent (Table 1). The neural spines of the vertebrae extend posterodorsally. All vertebrae as of the 5th vertebra (first free vertebra, Fig. 6) present a posterodorsally oriented accessory process with keel projections. The paired accessory processes progressively elongate and are closer to each other dorsoposteriorly to form the pseudoneural spines. The neural arches are fused from vertebra 15 or 16, resulting in the first neural spine. Pairs of pleural ribs are present from vertebra 5 to 14–15. Distal extremities of the pleural ribs are tapered. The parapophyses are long and tapered and with a spoon-like distal area for articulation of the pleural ribs (Table 1). The first complete haemal spine appears on vertebrae 16 or 17 (Table 1). The neural and haemal spines of the caudal vertebrae are roughly straight to slightly curved from the arch junction.

The elements of the homocercal caudal fin are described in Fig. 8.

Appendicular skeleton

The dorsal fin rays are supported by blade-like pterygiophores and fin rays (Fig. 6, Table 1). The proximal tip of the first pterygiophore of the dorsal fin is located between the bifid neural spine of the vertebra 4 (Fig. 6). The proximal tip location of the last pterygiophore is indicated in Table 1.

Skeletal elements of the pectoral and pelvic fin are described in Figs 9 and 10, respectively. The length of the pectoral fin rays related to the total length of the individual is indicated in Table 2. The rigid spine is long, wide and roughly straight, tapering distally, with the surface presenting numerous hooks. The number of fin rays is shown in Table 1.

The anterolateral arm of the basipterygium is located below the region of the vertebral *centra* 9, and the site of insertion of the pelvic fin ray is located below the region of vertebrae 13–14 in all specimens.

The location of anal and adipose fins is indicated in Table 1.

Skeletal anomalies

Although the characterization of skeletal anomalies was not the goal of the present study, noteworthy is that skeletal abnormalities were found in several specimens (that were not used to describe the normal skeletal anatomy). Most of these were located in the cranium and the axial skeleton and consisted of light anomalies such as deformed haemal and neural arches and spines, as well as severe anomalies such as vertebral compression (between vertebrae 15 and 20 and at the caudal fin complex), absence of the epiphyseal bar and impaired development of the lateral ethmoid (Fig. 11, Table 3).

Discussion

Normal skeletal anatomy

This study aimed at describing the normal bony skeleton of *P. punctifer* juveniles for use as a reference when assessing the adequacy of the nutritional and environmental conditions in experimental rearing during the early stages of development. In general, *P. punctifer* presents a bony skeleton typical of catfishes (Alexander, 1965; Diogo et al., 2001; Arratia, 2003a,b; Bockmann and Castro, 2010) with some particularities.

Head skeleton. As in all catfishes, the antorbital in *P. punctifer* connects with the autopalatine, maxilla and lateral ethmoid to participate in the movement of the maxillary barbel, enabling tasting the food (Alexander, 1965; Arratia, 2003a). However, the vomer does not contact the orbitosphenoid (as in Siluridae, Glyptosterninae and Trichomycteridae), as it does in other catfishes (Arratia, 2003a).

The hyomandibular and metapterygoid are connected in catfishes and present small eyes and a broad head. However, no sutural contact between the hyomandibular and metapterygoid was observed in *P. punctifer* at the studied developmental stage. Analysis of older specimens would determine whether they remain separated or finally connect. In some catfishes these elements are only connected through the quadrate (Adriaens, 1998; Arratia, 2003a).

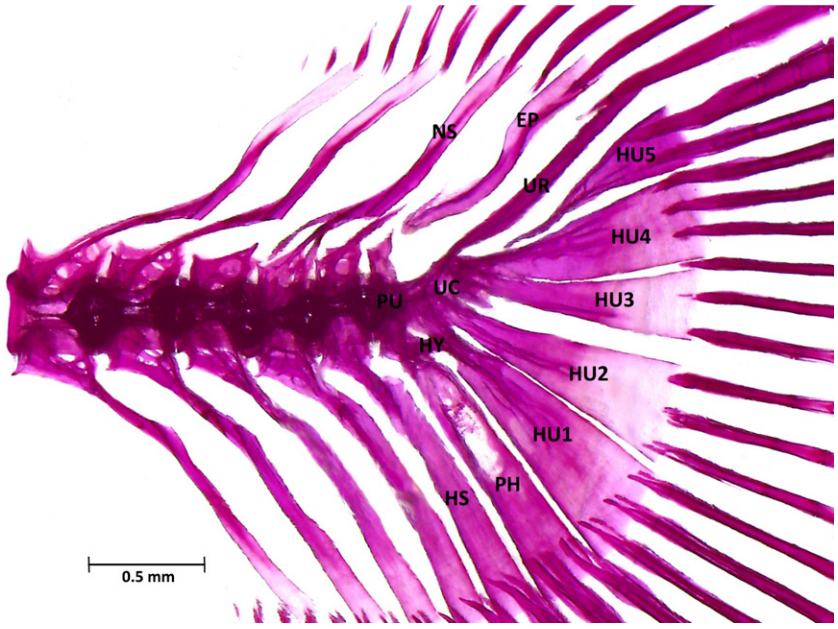

Fig. 8. Homocercal caudal fin of *Pseudoplatystoma punctifer*, 28 mm SL (reared at 28.3 ± 0.4°C), lateral view. HU1 and 2 similar, triangular and not fused. HU3 and 4 triangular and co-ossified anteriorly. HU5 triangular with the anterior part elongated. HU2 and 3 distinctly separated. Single EP, convex anterodorsally and concave posterodorsally. Two HY, one fused anterolaterally to the proximal part of PH and fused posterolaterally to the proximal part of HU1, the other joins HU1 and 2. PH and HU1 with a depression on their proximal part, below HY. Oval-shaped zone in the anteromedial region of PH weakly ossified. HU1 to 4 support 3 caudal rays each, HU5 supports 2. PU and UR totally co-ossified. Each HU's caudal ray articulated with HU. All caudal fin rays articulated on bony structures. HU5 and PH articulate the longer and larger caudal fin rays. On the dorsal lobe, caudal fin rays smaller from HU5 to HU3 and from HU5 to the neural arches of the last caudal vertebrae. On the ventral lobe, caudal fin rays smaller from PH to HU2 and from PH to the haemal arches of the last caudal vertebrae. Caudal fin rays without marginal expansions. EP, epural; HS, heamal spine; HU1-5, hypurals; HY, hypurapophysis; NS, neural spine; PH, parhypural; PU, preural; UC, ural centrum; UR, uroneural

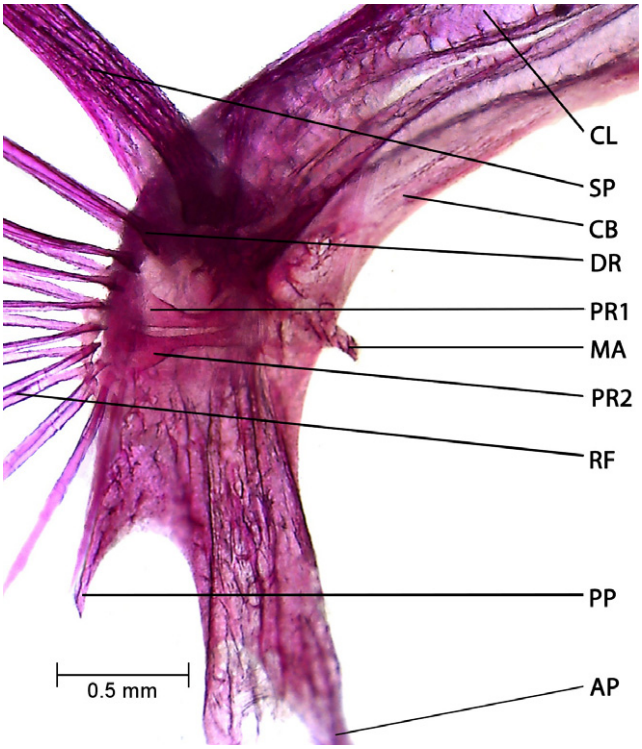

Fig. 9. Basal region of the right pectoral fin of *Pseudoplatystoma punctifer*, 28 mm SL (reared at 28.3 ± 0.4°C), ventral view. Ascending limb of AP wide and articulates between the ventrolateral and ventromedial limbs of the supracleithrum (not shown in figure). PP triangular, long and forms posteriorly a spine. MA wide. CL both united at the ventral midline by a ligamentous joint as well as the paired coracoids. Anterior part of CL with keel projections and wider than posterior part. Margins of CL mostly straight, although broadly concave lateroposteriorly. Coracoids interlocked by two sutural dentations. Coracoid keel shallow and concave at the inner lateral margin. PR1 and 2 rod-like, expanded to the extremities, especially the distal part, and completely ossified except for the cartilaginous extremities. PR2 slightly longer than PR1 with a wider distal tip. Rigid SP long, wide and roughly straight tapering distally. SP surface with numerous hooks. AP, articular cleithral process; CB, posterior complex bone of pectoral girdle (scapula, coracoid, and mesocoracoid fused); CL, cleithrum; DR, distal ray; MA, mesocoracoid arch; PP, postcleithral process; PR1-2, proximal radials 1 and 2; RF, ray fin; SP, pectoral spine

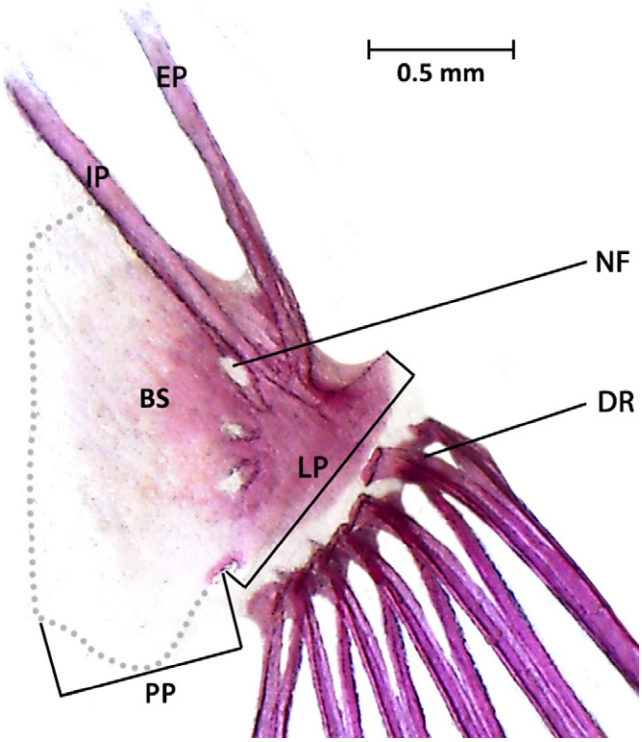

Fig. 10. Right pelvic fin of *Pseudoplatystoma punctifer*, 28 mm SL (reared at 28.3 ± 0.4°C), dorsal view. EP and IP of BS similar, long and roughly straight. BS not totally ossified. Lateral margin of PP of BS weakly ossified. Medial cartilage of paired BS fused on ventral midline. Posterolateral cartilage of BS distinctly separated from cartilage of PP of BS. Six pelvic fin rays present in all specimens (n = 10). Anterolateral arm of BS located below the region of vertebral *centra* 9 and site of insertion of pelvic fin ray below the region of the vertebrae 13–14. BS, basipterygium; DR, distal radial; EP, external anterior process (or anterolateral arm); IP, internal anterior process (or anteromedial arm); LP, lateral process; NF, neural foramen; PP, posterior process. Dotted line delimits the inner margin of BS

Table 2
Ratio pectoral fin ray length/SL measured on normal skeletons of reared *Pseudoplatystoma punctifer* juveniles (18.6 ± 1.5 mm SL; rearing temperature 28.3 ± 0.4°C, n = 10). Values are expressed in mean ± SD

Pectoral fin ray	Pectoral fin length/SL (mm)
1	0.27 ± 0.013
2	0.26 ± 0.009
3	0.19 ± 0.008
4	0.13 ± 0.006
5	0.09 ± 0.005
6	0.08 ± 0.003
7	0.07 ± 0.003
8	0.06 ± 0.003
9	0.02 ± 0.006

Pseudoplatystoma punctifer has two fontanels, similar to *Diplomystes camposensis* (Diplomystidae) and *Glyptosternon maculatum* (Sisoridae), whereas other catfishes present none, one or more than two fontanels (Arratia, 2003a). The length of sphenotic versus pterotic and frontal versus supraoccipital is variable between catfishes. In *P. punctifer* the perotic is longer than the sphenotic such as in *Silurus glanis* (Arratia, 2003a), and the supraoccipital is longer than the frontal, similar to *Arius*, *Otocinclus* and *Parapimelodus* (Arratia, 2003a). The bones surrounding the trigeminofacial foramen also vary among catfishes. The most common are the pterosphenoid and the prootic. In *P. punctifer* the pterosphenoid, parasphenoid, sphenotic and prootic surround the foramen, as is also the case of *Chrysichthys* (Arratia, 2003a).

Axial skeleton. The Weberian apparatus is believed to improve the mechanical connection of the swim bladder with the labyrinths and serves to ameliorate audition, an

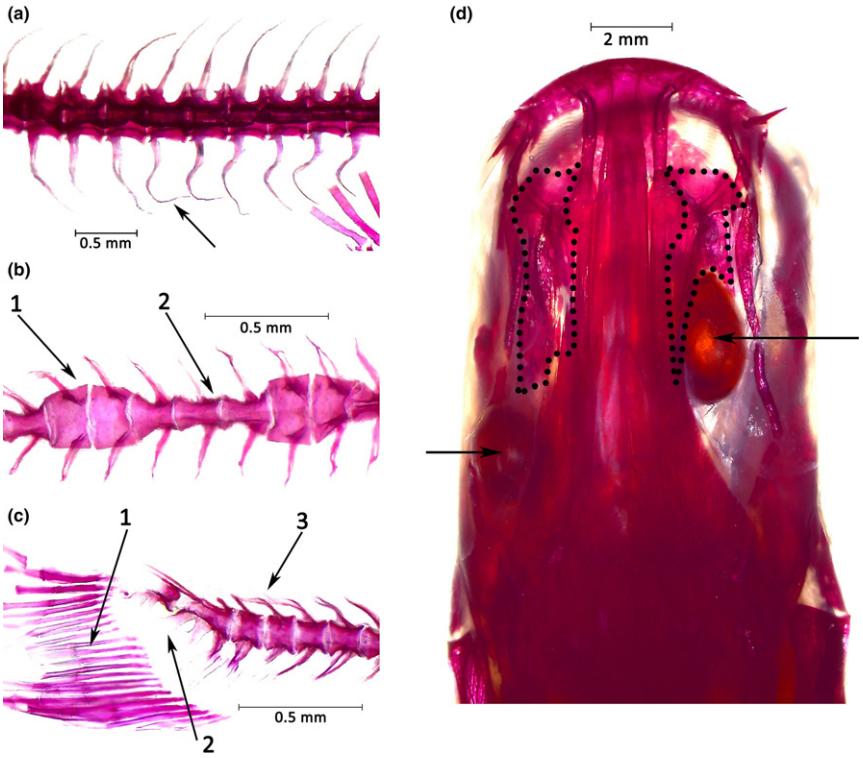

Fig. 11. Skeletal anomalies in *Pseudoplatystoma punctifer* reared at 28.3 ± 0.4°C. (a, b) Lateral view of haemal vertebrae. (a) 20 mm SL, arrow shows deformed haemal arches. (b) 12 mm SL, arrow 1 shows lateral compressions of the vertebrae and arrow 2 indicates dorsoventral compressions of the vertebrae. (c) Lateral view of the caudal fin complex, 12 mm SL. Arrow 1 shows deformed caudal fin rays, arrow 2 deformed hypurals and arrow 3 deformed neural arches. (d) Dorsal view of the skull, 47 mm SL. Arrows indicate the position of the eyes and dotted lines delimit the lateral ethmoid

Table 3
Frequency and type of skeletal anomalies found in reared *Pseudoplatystoma punctifer* juveniles (23.2 ± 5.5 mm SL; rearing temperature 28.3 ± 0.4°C, n = 18)

Skeletal anomalies	Frequency (%)
Severe anomalies	
Vertebral compression	11
Absence of the epiphyseal bar	16
Light anomalies	
Anomalies in haemal and neural arches and spines	55

advantageous characteristic in relation to poor vision (Chardon et al., 2003). The main differences of the Weberian ossicles among catfishes are found in the processes of the intercalarium and scaphium and the ossa suspensoria. For instance, the intercalarium is absent in *P. punctifer* as in other catfishes, such as in some silurids, clariids and loricarioids. In many other catfishes it is reduced to an intraligamentous ossification (Chardon et al., 2003). As in all catfishes, the first vertebra is reduced to its *centra* and the vertebrae 2–4 are fused to form the complex centrum or complex vertebra. The supraneural and proximal radials are sutured together in *P. punctifer* and the pterygophore 1 and 2 are fused distally by a bony bridge that allows the neural spine of the vertebra 4 to move only anteroposteriorly. A similar configuration has been found in *Pimelodus* and *Diplomystes* (Alexander, 1965).

The vertebral column of catfishes is composed of a variable number of vertebrae, the most common being between 40 and 50 (i.e. Aridae, Bagridae, Ictaluridae), although lower and higher numbers of vertebrae are also found (15–29 in Pangasidae and 56 to over 100 in Clariidae) (Arratia, 2003b). *Pseudoplatystoma punctifer* presents 43–44 vertebrae, 44 being the most frequent number, and the tip of the first pterygiophore placed between the haemal spines of vertebrae 23–26, being between vertebrae 24 and 25 as the most frequent point. However, these skeletal features found in the present study do not coincide with the *P. punctifer* description reported in a systematic review of the genus *Pseudoplatystoma* that defined eight species based on morphological characters, whereby *P. punctifer* presented 37–40 vertebrae and the first spinelet of the anal fin contacts the haemal arch of vertebra 22 (Buitrago-Suárez and Burr, 2007). The individuals used in our study were obtained from a broodstock originating from the Iquitos region (Peru) and identified as *P. punctifer* according to the morphological (colour pattern) and the geographical distribution description of Buitrago-Suárez and Burr (2007); according to their key to the genus *Pseudoplatystoma*, the species that presents 43–45 vertebrae and in which the first spinelet of the anal fin contacts the haemal arch of vertebra 24 corresponds to *P. fasciatum*, a species they considered as restricted to the Guyana region.

After the Buitrago-Suárez and Burr (2007) revision, two molecular phylogenies of the genus *Pseudoplatystoma* revealed no differences between *P. punctifer* and *P. fasciatum* (Torrico et al., 2009; Carvalho-Costa et al., 2011). More recently, a molecular study conducted in the region of Iquitos proposed that two different species might exist within the *P. punctifer* clade, the Guyana sequence of *P. fasciatum* being nested inside one of the two identified clusters and to which the broodstock used in this study corresponds (García-Dávila et al., 2013). In view of the skeletal differences found between the results of the present study and the key to the genus of Buitrago-Suárez and Burr (2007) further studies on this genus are necessary.

The caudal fin complex of *P. punctifer* is also characteristic of catfishes. The presence of the hypurapophysis is correlated with certain environmental conditions (i.e. water speed) (Arratia, 2003b).

Appendicular skeleton. There is a reduction in the number of bones of the pectoral girdle in catfishes, either by fusion or loss of elements. The four proximal pectoral radials of primitive teleosts are reduced to three or two, the latter being the case of *P. punctifer*. There are six pelvic fins in *P. punctifer*, such as in other catfishes. However, more than six are also found in some doradids, synodontids or silurids (Arratia, 2003b). The pelvic fins have a variety of functions depending on the catfish species, the most common serving for stabilizing and turning the body (Arratia, 2003b). *Pseudoplatystoma punctifer* presents pectoral and dorsal spines, considered a synapomorphy of Siluriformes. Their main function is protective, as they can be erected and locked, thus making it difficult for predators to manipulate and swallow them (Alexander, 1965).

The adipose fin is well developed in *P. punctifer*, as in bagrids. The size of the adipose fin is variable or even missing among catfishes (Arratia, 2003b).

Skeletal anomalies

Several skeletal anomalies were observed in *P. punctifer*, indicating that rearing conditions might have been suboptimal. Many factors have been considered as being a cause of these skeletal anomalies, such as colour, shape and volume of tank, stocking density, oxygen level, water quality, light intensity and duration, water temperature and nutrition (Boglione et al., 2013a,b). It is also known that several causative factors can induce the same skeletal anomaly, and that the same causative factor can induce several skeletal anomalies in different fish species (Boglione et al., 2013a) and that sensitivity to a certain causative factor can change during ontogeny (Mazurais et al., 2009; Darias et al., 2010b, 2011a,b).

Although skeletal anomalies can appear at any time of the fish lifecycle, most have their onset during larval development, when the ontogenesis of the skeletal system takes place (Darias et al., 2010b, 2011a,b; Boglione et al., 2013a). Eye asymmetry has been observed in *P. punctifer* adults (M. J. Darias, personal observation); we found this morphological abnormality in juveniles during our study and observed that it was correlated with an anomaly of the lateral ethmoid of the neurocranium, which serves to protect the eye anteriorly. It needs to be determined whether this abnormality is due to an alteration during cell differentiation and leading to a deformed skeletal element or to a disruption that occurred during the ossification process of the lateral ethmoid. In several species, the lateral ethmoid is one of the first structures of the ethmoid region to ossify (Faustino and Power, 2001). An alteration of the ossification process during the early ontogeny of *P. punctifer* could lead to an incorrect location of the eye. In general, the appearance of skeletal anomalies in early juveniles of *P. punctifer* could indicate that their origin might be found during skeletal tissue differentiation. Further research on the ontogeny of the skeletal development of this species will help to precociously diagnose skeletal abnormalities and to better understand their origin by studying the effects of different environmental and/or nutritional factors on skeletogenesis.

Acknowledgements

This work was funded by the International Joint Laboratory 'Evolution and Domestication of Amazonian Ichthyofauna' (LMI EDIA, IRD-IIAP). Guillain Estivals was supported by the French Ministry of Foreign Affairs (International Volunteer contract).

References

Adriaens, D., 1998: On how a larva becomes an adult catfish. Doctoral thesis, Gant University, Belgium, 240 pp.

Alexander, R. McN., 1965: Structure and function in the catfish. J. Zool. **148**, 88–152.

Arratia, G., 2003a: Catfish head skeleton – an overview. In: Catfishes. G. Arratia, A. S. Kapoor, M. Chardon and R. Diogo (Eds). Science Publishers, Enfield, pp. 3–46.

Arratia, G., 2003b: The siluriform postcranial skeleton – an overview. In: Catfishes. G. Arratia, A. S. Kapoor, M. Chardon and R. Diogo (Eds). Science Publishers, Enfield, pp. 121–157.

Baras, E.; Silva del Aguila, D. V.; Montalvan Naranjos, G. V.; Dugué, R.; Chu Koo, F.; Duponchelle, F.; Renno, J. F.; Garcia-Dávila, C.; Nuñez, J., 2011: How many meals a day to minimize cannibalism when rearing larvae of the Amazonian catfish *Pseudoplatystoma punctifer*? The cannibal's point of view. Aquat. Living Resour. **24**, 379–390.

Bockmann, F. A.; Castro, R. M. C., 2010: The blind catfish from the caves of Chapada Diamantina, Bahia, Brazil (Siluriformes: Heptapteridae): description, anatomy, phylogenetic relationships, natural history, and biogeography. Neotrop. Ichthyol. **8**, 673–706.

Boglino, A.; Wishkerman, A.; Darias, M. J.; Andree, K. B.; de la Iglesia, P.; Estévez, A.; Gisbert, E., 2013: High dietary arachidonic acid levels affect the process of eye migration and head shape in pseudoalbino Senegalese sole *Solea senegalensis* early juveniles. J. Fish Biol. **83**, 1302–1320.

Boglione, C.; Gavaia, P.; Koumoundouros, G.; Gisbert, E.; Moren, M.; Fontagné, S.; Witten, P. E., 2013a: Skeletal anomalies in reared European fish larvae and juveniles. Part 1: normal and anomalous skeletogenic processes. Rev. Aquac. **5**, 99–120.

Boglione, C.; Gisbert, E.; Gavaia, P.; Witten, P. E.; Moren, M.; Fontagné, S.; Koumoundouros, G., 2013b: Skeletal anomalies in reared European fish larvae and juveniles. Part 2: main

typologies, occurrences and causative factors. Rev. Aquac. **5**, 121–167.

Buitrago-Suárez, U. A.; Burr, B. M., 2007: Taxonomy of the catfish genus *Pseudoplatystoma* Bleeker (Siluriformes: Pimelodidae) with recognition of eight species. Zootaxa **38**, 1–38.

Cahu, C.; Zambonino-Infante, J.; Takeuchi, T., 2003: Nutritional components affecting skeletal development in fish larvae. Aquaculture **227**, 245–248.

Carvalho-Costa, L. F.; Piorski, N. M.; Willis, S. C.; Galetti, P. M.; Ortí, G., 2011: Molecular systematics of the neotropical shovelnose catfish genus *Pseudoplatystoma* Bleeker 1862 based on nuclear and mtDNA markers. Mol. Phylogenet. Evol. **59**, 177–194.

Chardon, M.; Parmentier, E.; Vandewalle, P., 2003: Morphology, development and evolution of the Weberian apparatus in catfish. In: Catfishes. G. Arratia, A. S. Kapoor, M. Chardon and R. Diogo (Eds). Science Publishers, Enfield, pp. 71–120.

Darias, M. J.; Lan Chow Wing, O.; Cahu, C.; Zambonino-Infante, J. L.; Mazurais, D., 2010a: Double staining protocol for developing European sea bass (*Dicentrarchus labrax*) larvae. J. Appl. Ichthyol. **26**, 280–285.

Darias, M. J.; Mazurais, D.; Koumoundouros, G.; Glynatsi, N.; Christodoulopoulou, S.; Huelvan, C.; Desbruyeres, E.; Le Gall, M. M.; Quazuguel, P.; Cahu, C. L.; Zambonino-Infante, J. L., 2010b: Dietary vitamin D3 affects digestive system ontogenesis and ossification in European sea bass (*Dicentrachus labrax*, Linnaeus, 1758). Aquaculture **298**, 300–307.

Darias, M. J.; Mazurais, D.; Koumoundouros, G.; Cahu, C. L.; Zambonino-Infante, J. L., 2011a: Overview of vitamin D and C requirements in fish and their influence on the skeletal system. Aquaculture **315**, 49–60.

Darias, M. J.; Mazurais, D.; Koumoundouros, G.; Le Gall, M. M.; Huelvan, C.; Desbruyeres, E.; Quazuguel, P.; Cahu, C. L.; Zambonino-Infante, J. L., 2011b: Imbalanced dietary ascorbic acid alters molecular pathways involved in skeletogenesis of developing European sea bass (*Dicentrarchus labrax*). Comp. Biochem. Physiol. A Mol. Integr. Physiol. **159**, 46–55.

Darias, M. J.; Castro-Ruiz, D.; Estivals, G.; Quazuguel, P.; Fernández-Méndez, C.; Nuñez, J.; Clota, F.; Gilles, S.; García-Dávila, C.; Gisbert, E.; Cahu, C., 2015: Influence of dietary protein and lipid levels on growth performance and the incidence of cannibalism in *Pseudoplatystoma punctifer* (Castelnau, 1855) larvae and early juveniles. J. Appl. Ichthyol.**31**: (suppl 4), 74–82.

Diogo, R.; Oliveira, C.; Chardon, M., 2001: On the homologies of the skeletal components of catfish (Teleostei: Siluriformes) suspensorium. Belg. J. Zool. **131**, 93–109.

Divanach, P.; Boglione, C.; Menu, B.; Koumoundouros, G.; Kentouri, M.; Cautadella, S., 1996: Abnormalities in finfish mariculture: an overview of the problem, causes and solutions. Seabass and Seabream Culture: Problems and Prospects. Handbook of Contributions and Short Communications. Verona, Italy, pp. 45–51.

Estivals, G.; Castro-Ruiz, D.; Fernández, C.; Núñez, J.; García-Dávila, C.; Duponchelle, F.; Renno, J. F.; Darias, M. J., 2015: Osteological development of reared *Pseudoplatystoma punctifer* with notes on the incidence of skeletal deformities. p. 58. In: 4th RIIA International Conference – Research Network on Amazonian Ichthyofauna: Book of Abstracts. M. J. Darias and D. Rejas (Eds). Universidad Mayor de San Simón; Institut de Recherche pour le Développement, Cochabamba; Marseille, 84 pp.

Faustino, M.; Power, D. M., 2001: Osteologic development of the viscerocranial skeleton in sea bream: alternative ossification strategies in teleost fish. J. Fish Biol. **58**, 537–572.

Fujimoto, R. Y.; Carneiro, D. J., 2008: Adição de ascorbil polifosfato, como fonte de vitamina C, em dietas para alevinos de pintado, *Pseudoplatystoma corruscans* (Agassiz, 1829) [Adding ascorbyl polyphosphate as a source of vitamin C in the diet of fingerlings of Pintado *Pseudoplatystoma corruscans* (Agassiz, 1829)]. Acta Sci. Anim. Sci. **23**, 855–861.

Fujimoto, R. Y.; Santos, R. F.; Carneiro, D. J., 2013: Morphological deformities in the osseous structure in spotted sorubim *Pseudoplatystoma coruscans* (Agassiz & Spix, 1829) with vitamin C deficiency. An. Acad. Bras. Ciênc. **85**, 379–384.

García-Dávila, C.; Duponchelle, F.; Castro-Ruiz, D.; Villacorta, J.; Quérouil, S.; Chota-Macuyama, W.; Núñez, J.; Römer, U.; Carvajal-Vallejos, F.; Renno, J. F., 2013: Molecular identification of a cryptic species in the Amazonian predatory catfish genus *Pseudoplatystoma* (Bleeker, 1962) from Peru. Genetica **141**, 347–358.

Gisbert, E.; Moreira, C.; Castro-Ruiz, D.; Oztürk, S.; Fernández, C.; Gilles, S.; Nuñez, J.; Duponchelle, F.; Tello, S.; Renno, J.-F.; García-Dávila, C.; Darias, M. J., 2014: Histological development of the digestive system of the Amazonian pimelodid catfish *Pseudoplatystoma punctifer*. Animal **8**, 1765–1776.

Kossowski, C., 1996: Perspectives de l'élevage des poissons-chats (Siluroidei) en Amérique du Sud [Perspectives of the breeding of catfishes (Siluroidei) in South America]. Aquat. Living Resour. **9**, 189–195.

Lall, S. P.; Lewis-McCrea, L. M., 2007: Role of nutrients in skeletal metabolism and pathology in fish – an overview. Aquaculture **267**, 3–19.

Lopes, T. D. S.; de Freitas, T. M.; Jomori, R. K.; Carneiro, D. J.; Portella, M. C., 2014: Skeletal anomalies of pacu, *Piaractus mesopotamicus*, larvae from a wild-caught broodstock. J. World Aquac. Soc. **45**, 15–27.

Mazurais, D.; Glynatsi, N.; Darias, M. J.; Christodoulopoulou, S.; Cahu, C. L.; Zambonino-Infante, J. L.; Koumoundouros, G., 2009: Optimal levels of dietary vitamin A for reduced deformity incidence during development of European sea bass larvae (*Dicentrarchus labrax*) depend on malformation type. Aquaculture **294**, 262–270.

Nuñez, J.; Dugué, R.; Corcuy Arana, N.; Duponchelle, F.; Renno, J.-F.; Raynaud, T.; Hubert, N.; Legendre, M., 2008: Induced breeding and larval rearing of Surubí, *Pseudoplatystoma fasciatum* (Linnaeus, 1766), from the Bolivian Amazon. Aquac. Res. **39**, 764–776.

Rasband, W. S., 1997–2012: ImageJ. US National Institutes of Health, Bethesda. Available at: http://imagej.nih.gov/ij/ (accessed on 4 September 12).

Torrico, J. P.; Hubert, N.; Desmarais, E.; Duponchelle, F.; Nuñez Rodriguez, J.; Montoya-Burgos, J.; Garcia Davila, C.; Carvajal-Vallejos, F. M.; Grajales, A. A.; Bonhomme, F.; Renno, J. F., 2009: Molecular phylogeny of the genus *Pseudoplatystoma* (Bleeker, 1862): biogeographic and evolutionary implications. Mol. Phylogenet. Evol. **51**, 588–594.

Author's address: Maria J. Darias, Institut de Recherche pour le Développement (IRD), UMR 207 BOREA, 911, Avenue Agropolis, BP 64501, F-34394 Montpellier Cedex 5, France.
E-mail: maria.darias@ird.fr